Ab initio density functional theory study on the atomic and electronic structure of GaP/Si(001) heterointerfaces

O. Romanyuk,[1,*] O. Supplie,[2] T. Susi,[3] M. M. May,[4] and T. Hannappel[2]

[1]*Institute of Physics, Academy of Sciences of the Czech Republic, Cukrovarnická 10, 16200 Prague, Czech Republic*

[2]*Institute of Physics, Department for Photovoltaics, TU Ilmenau, Gustav-Kirchhoff-Straße 5, 98693 Ilmenau, Germany*

[3]*Faculty of Physics, University of Vienna, Boltzmanngasse 5, 1090 Vienna, Austria*

[4]*Department of Chemistry, University of Cambridge, Lensfield Road, Cambridge, United Kingdom*

The atomic and electronic band structures of GaP/Si(001) heterointerfaces were investigated by *ab initio* density functional theory calculations. Relative total energies of abrupt interfaces and mixed interfaces with Si substitutional sites within a few GaP layers were derived. It was found that Si diffusion into GaP layers above the first interface layer is energetically unfavorable. An interface with Si/Ga substitution sites in the first layer above the Si substrate is energetically the most stable one in thermodynamic equilibrium. The electronic band structure of the epitaxial GaP/Si(001) heterostructure terminated by the (2×2) surface reconstruction consists of surface and interface electronic states in the common band gap of two semiconductors. The dispersion of the states is anisotropic and differs for the abrupt Si-Ga, Si-P, and mixed interfaces. Ga $2p$, P $2p$, and Si $2p$ core-level binding-energy shifts were computed for the abrupt and the lowest-energy heterointerface structures. Negative and positive core-level shifts due to heterovalent bonds at the interface are predicted for the abrupt Si-Ga and Si-P interfaces, respectively. The distinct features in the heterointerface electronic structure and in the core-level shifts open new perspectives in the experimental characterization of buried polar-on-nonpolar semiconductor heterointerfaces.

I. INTRODUCTION

GaP/Si(001) is an attractive quasisubstrate for III/V-on-Si integration, which is highly desired for microelectronics [1], high-efficiency photovoltaics, and water-splitting devices [2]. In such polar-on-nonpolar heterostructures, the heterointerface is of particular interest since its atomic and electronic structure highly impacts crystal quality and the efficiency of the devices. Preparation of sharp and well-ordered interfaces is desirable in device growth technology. However, there are many factors that influence the sharpness of grown heterointerfaces [3], such as charge accumulation [4] and antiphase domain boundaries (ADBs) at heterointerfaces due to monoatomic steps on the Si(001) substrate [5]. The ADB density can be reduced if a single-domain Si(001) substrate is used [5,6]. The mechanism of charge compensation at the heterovalent GaP/Si interface is not yet completely understood and therefore it cannot be controlled during epitaxy.

The valency of dissimilar materials at the heterointerface is an important parameter influencing interface sharpness and charge accumulation [3]. In particular for GaP/Si, the partial electronic charge for one heterovalent Si-P or Si-Ga bond is 1+5/4 or 1+3/4 electrons, respectively. Since one bond consists of two electrons, every heterovalent Si-P or Si-Ga bond donates 1/4 or accepts 1/4 electrons. In contrast to isovalent interfaces, charge accumulates in the near-interface region, and a huge electric field is expected at abrupt interfaces [4,7] consisting of only Si-P bonds for the P-polar interface and only Si-Ga bonds for the Ga-polar interface. Charge neutrality at the interface can be achieved in arbitrarily thick mixed GaP/Si layers if the number of Si-P bonds is equal to the number of Si-Ga bonds in mixed interfacial layers.

The stability of abrupt and mixed GaP(001)-(2×2)/Si(001) interfaces was investigated recently [6]. Charge-neutral (compensated) interfaces were suggested by allowing atomic intermixture within *one* interfacial bilayer (similar to the models suggested by Harrison *et al.* [4]). It was found that the energetically most favorable interface consists of a Si/Ga mixed layer, whereas the formation of the Si/P mixed interface requires a higher interface energy. Nevertheless, both compensated interfaces have lower energies than their abrupt interface counterparts. GaP/Si intermixing within more than one layer above the interface has not been investigated by density functional theory (DFT) so far.

Besides energetic considerations, kinetic processes play an important role during GaP growth on Si. The formation of a heterointerface at elevated temperature depends on numerous aspects such as preferred binding sites, the mobility of atoms at the terraces, step height, and density, as well as process routes [8]. In particular, a typical, relatively fast pulsed nucleation during metal-organic chemical-vapor deposition (MOCVD) cannot be considered an equilibrium process. The interface formation may be kinetically limited and interface structures may be "frozen" during further processing so that the energetically lowest structures are not necessarily realized. One famous example is the kinetically driven anomalous formation of the energetically unfavored (1×2) reconstructed Si(001) surface on $2°$ misoriented substrates in H_2 ambient [9].

Recently, a strong prevalence of Si-P bonds in the GaP thin film on a Si(001) substrate was revealed by x-ray photoelectron spectroscopy (XPS) [10]. Similarly, Si-As bonds were found at the GaAs/Si(001) heterointerface [11]. It was also observed that Si-Ga bonds become more favorable in more Ga-rich nucleation conditions [6,10].

*romanyuk@fzu.cz

Other recent work suggested the formation of pyramidal structures with different facets at the GaP/Si(001) heterointerface based on transmission electron spectroscopy (TEM) measurements and theoretical analysis [12]. DFT calculation results in this work are questionable, however, since the interface energy depends on the chemical potentials, i.e., the stoichiometry of interfacial structure models, which was not considered there. In addition, the interface energies computed in Ref. [12] seem to consist of surface energy contributions from P-H and Ga-H bonds, which is different for different facets [13]. Therefore, the GaP/Si(001) interface structure and thickness of potentially intermixed interfacial layers, i.e., the prevailing interface stoichiometry after the entire GaP epilayer growth, remains an open question.

On the other hand, the presence of interface-state dispersion in the electronic band structure could yield direct experimental evidence of atomically well ordered bonding configurations at the heterointerface. Ordered heterovalent interfaces can be considered two-dimensional objects similar to the surfaces of solids. Electronic surface states exhibit two-dimensional dispersion relations, which can be experimentally determined by angle-resolved photoemission spectroscopy (ARPES), for instance. The measurements of buried interface states by photoemission techniques are not straightforward [14], however, due to the limited inelastic mean free path (IMFP) of photoelectrons. Alternative techniques such as reflection anisotropy spectroscopy (RAS) [15,16], transport measurements [17,18], or electron-energy-loss spectroscopy [19] (EELS) in combination with scanning transmission electron microscopy [3] (STEM) are also promising to analyze the interfacial electronic structure.

Localized electronic states may originate from substitutional site defects, vacancies, or heterovalent bonds at the interface. Interface states were predicted in the fundamental band gap for heterovalent heterostructures such as GaAs/Ge [20], GaAs/Si [21], and ZnSe/Ge [22]. The electronic band structure of GaAs/ZnSe [15] and ZnSe/Ge [23] heterostructures have also been investigated experimentally. Particularly for ZnSe/Ge, it was found that localized interface states are not present for abrupt interfaces, but appear as a result of substitution sites in interfacial layers [24].

In the present paper, the atomic structure and electronic band structure of the GaP/Si(001) heterostructure are investigated. The number of known interface models [6] is extended by allowing atomic intermixture within three GaP bilayers above the interface. Atomic slabs consisting of surfaces are used rather than superlattices [25] in order to simulate more realistic epitaxial films and to exclude internal field modulation due to polar interfaces. The core-level binding-energy shifts and interface-state dispersion are derived for both abrupt and mixed GaP/Si(001) interfaces.

II. COMPUTATIONAL DETAILS

The total energy calculations of GaP/Si(001) interface models were carried out using the ABINIT computer code [26,27]. The generalized gradient approximation (GGA) for the exchange-correlation energy functional was used. Norm-conserving pseudopotentials [28] of the Troullier-Martins type [29] were used to describe the atomic species. The electronic
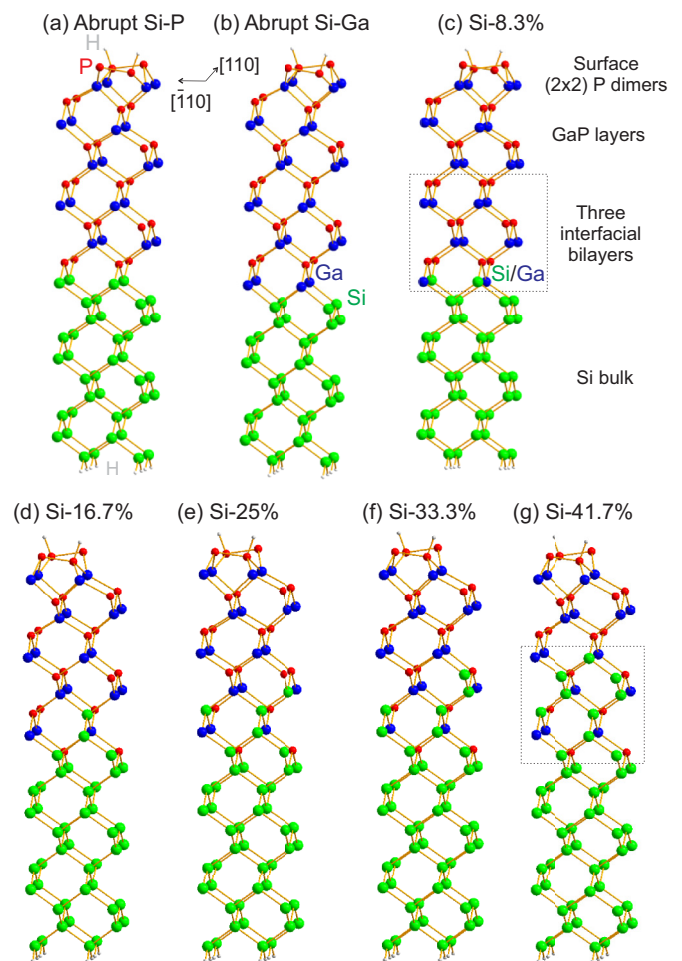

FIG. 1. Structure models of selected GaP/Si(001) heterointerfaces. GaP layers are terminated by the (2×2) surface reconstruction consisting of P dimers and H. Abrupt interfaces consist of (a) Si-P and (b) Si-Ga bonds. Si substitutional sites are present in up to three interfacial bilayers at mixed interfaces. The Si concentration in the interfacial layers is used for model notations in (c)–(g). Si, Ga, and P atoms are marked in green, blue, and red, respectively.

wave functions were expanded in a plane-wave basis with a kinetic energy cutoff of 12 hartrees. The **k**-point sets [30] corresponding to $6 \times 6 \times 1$ points per (2×2) unit cell were used. Atomic slabs were constructed using the repeated supercell approach with a slab thickness of 30 Å and a vacuum gap region of 19 Å.

A few test calculations with semicore Ga $3d$ electrons were carried out. The converged value of kinetic energy cutoff was increased up to 30 hartrees in this case. However, only small differences in interface stabilities [less than 0.02 eV/(1×1)] and electronic band structures (less than 0.1 eV) were observed, which we consider negligible in the following.

The GaP(001) surface can be terminated by either Ga-P or P-P dimers [31,32]. The P-rich surface reconstruction consists of two buckled P-P dimers and one H atom per dimer, which arrange in rows causing (2×2) or $c(4 \times 2$) reconstructions [31,32]. In the present work, all slabs were terminated by the same P-rich GaP(001)-(2×2) surface reconstruction (Fig. 1), whereas the interface structure was varied. The influence of

surface atomic relaxations on the interface atomic structure was found to be negligible.

The equilibrium lattice constant for relaxed bulk Si ($a_{\text{Si}} = 5.46$ Å) was used in the calculations. Band-gap energies of 0.66 and 1.69 eV were derived for bulk Si and bulk GaP, respectively. These values are about 0.5 eV smaller than the experimental values due to the well-known band-gap problem. While this does not affect the valence-band offset (VBO) calculations, an uncertainty up to 0.5 eV should be taken into account for the alignment of the interface states within the common band gap of heterostructures.

The bottom Si layer of the slab was passivated by H atoms. Atomic coordinates of the slab were relaxed until interatomic forces became smaller than 10^{-3} hartrees/bohr, whereby only the two Si bottom layers and one H layer were kept fixed.

The relative interface formation energy $\Delta\gamma$ was expressed as follows [33]:

$$\Delta\gamma A = E - n_{\text{Ga}}\mu_{\text{Ga}} - n_P\mu_P - n_{\text{Si}}\mu_{\text{Si}}, \quad (1)$$

$$E = E_{\text{tot}} - E_{\text{ref}}, \quad (2)$$

where E_{tot} is the total energy of the slab and E_{ref} is the reference energy of a thinner slab excluding three GaP bilayers. E_{ref} is identical for all models and includes the (2×2) surface reconstruction energy. μ_i is the chemical potential of species i, n_i is the number of atoms of the ith species in the mixed layer, and A is the interface unit-cell area.

In thermodynamic equilibrium, the Ga, P, and Si chemical potentials are equal to the corresponding values of chemical potentials in a bulk:

$$\mu_{\text{GaP}}^{\text{bulk}} = \mu_{\text{Ga}} + \mu_P, \quad (3)$$

$$\mu_{\text{Si}}^{\text{bulk}} = \mu_{\text{Si}}. \quad (4)$$

The variation of μ_{Ga} and μ_P at the interface was limited to the corresponding bulk chemical potentials $\mu_{\text{Ga}}^{\text{bulk}}$ and μ_P^{bulk}. The boundary conditions were expressed as follows:

$$H_f^{\text{GaP}} + \mu_P^{\text{bulk}} \leqslant \mu_P \leqslant \mu_P^{\text{bulk}}, \quad (5)$$

where $H_f^{\text{GaP}} = \mu_{\text{GaP}}^{\text{bulk}} - \mu_{\text{Ga}}^{\text{bulk}} - \mu_P^{\text{bulk}}$ is the heat of formation. The bulk chemical potentials, $\mu_{\text{Ga}}^{\text{bulk}}$ and μ_P^{bulk}, were calculated for the orthorhombic α-Ga phase [34] and the orthorhombic black P phase [35], respectively. The computed value of the heat of formation for GaP, $H_f^{\text{GaP}} = -0.86$ eV, is similar to the value reported in the literature [36]. Finally, the relative interface energy $\Delta\gamma$ can be expressed as follows [33]:

$$\Delta\gamma A = E - (n_P - n_{\text{Ga}})\Delta\mu_P - n_P\mu_{\text{GaP}}^{\text{bulk}} - n_{\text{Si}}\mu_{\text{Si}}^{\text{bulk}}, \quad (6)$$

$$\Delta\mu_P = \mu_P - \mu_P^{\text{bulk}}, \quad (7)$$

where the chemical potential variation boundaries are $\Delta\mu_P/H_f^{\text{GaP}} = -1$ for Ga-rich conditions and $\Delta\mu_P/H_f^{\text{GaP}} = 0$ for P-rich conditions.

It should be noted that the relative interface energies are sufficient for the present analysis, i.e., the analysis of the (001)-oriented heterostructure. In the case of multiple facets [12], absolute energies of polar interfaces [37,38] have to be

computed and used for comparison. Such analysis is out of the scope of the present paper, however.

Relaxed atomic positions of GaP/Si(001) heterostructure models were used for the core-level binding energies and electronic band structure calculations. In order to identify surface and interface states, wave functions of the relaxed structures were derived using the CUT3D utility of the ABINIT program.

The Ga $2p_{3/2}$, P $2p_{3/2}$, and Si $2p_{3/2}$ core-level binding energies of atoms at interfaces and in the "bulk" (in GaP and Si layers above and below the interface) were computed for three interface models. The delta Kohn-Sham (ΔKS) method [39,40] within the grid-based projector-augmented wave (PAW) code GPAW [41] was used, which enables highly parallel and efficient core-level calculations. In this method, the core-level binding energy is the total energy difference between the ground state and the first core-ionized state, explicitly introduced for each element via a PAW data set with its $2p_{3/2}$ occupancy reduced by one electron. A compensating electron charge is introduced in the conduction band to ensure charge neutrality and to model the screening of the core hole. Exchange and correlation were estimated by the Perdew-Burke-Ernzerhof (PBE) generalized gradient approximation and Monkhorst-Pack $12 \times 12 \times 1$ **k**-point meshes used to sample the Brillouin zone (several binding-energy values were checked with a larger $16 \times 16 \times 1$ **k**-point set, and no difference within our computation accuracy was observed). Spin-orbit splitting is not included in the calculation since similar shifts for $2p_{3/2}$ and $2p_{1/2}$ peak pairs are expected.

III. RESULTS AND DISCUSSION

A. Interface atomic structure

The number of possibilities for Si substitutional sites within a few GaP interfacial layers is very large. In order to limit the number of models, Si/Ga and Si/P substitution sites were allowed only in the three GaP bilayers above the interface (vacancy defects were not considered). Previous studies have shown that charge-compensated interfaces are energetically more favorable than uncompensated interfaces. Therefore, we compute only structures which obey the electron counting model [42] (ECM). For interfaces, the ECM can be expressed as the sum of partial charges of bonds times the number of corresponding Si-P, Si-Ga, Ga-Ga, and P-P bonds:

$$\frac{1}{4}(N_{\text{Si-Ga}} - N_{\text{Si-P}}) + \frac{1}{2}(N_{\text{Ga-Ga}} - N_{\text{P-P}}) = 0, \quad (8)$$

where N_{i-j} is the number of $i - j$ bonds and $\frac{1}{4}$, $\frac{1}{2}$ are the partial charges of the corresponding bonds. Ga-P or Si-Si bonds do not produce partial charge and therefore were not included in Eq. (8).

Furthermore, the Si occupancy in each monolayer was limited to 50%. A larger Si concentration can hardly be achieved without additional Si flux supply or temperatures high enough to support Si diffusion from the bulk. The Si concentration was estimated as $c_{\text{Si}} = 100 \times n_{\text{Si}}/24$, where n_{Si} is the number of Si substitution sites at $3 \times (2 \times 2) = 24$ possible positions in the three GaP bilayers above the Si substrate. This leads to 91 nonequivalent compensated interface models for each of the Si-P and Si-Ga interfaces.
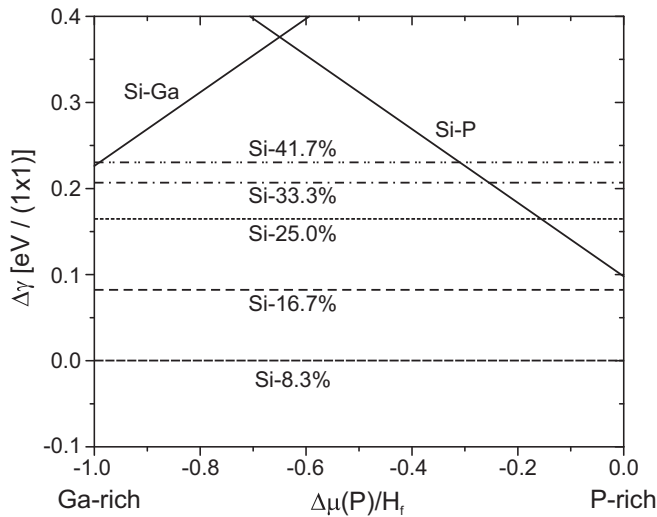
FIG. 2. Relative total interface energy diagram for GaP/Si(001) with different interface structures. Atomic structures of the models are shown in Fig. 1. The lowest interface energy (Si-8.3% model) was set to zero. The interface energy increases with Si concentration in the GaP layers. The abrupt Si-P and Si-Ga interfaces have higher energy than the compensated mixed interfaces in thermodynamic equilibrium.

FIG. 3. Averaged electrostatic potential $\bar{V}$ of the (a) abrupt Si-P, (b) abrupt Si-Ga, and (c) mixed Si-8.3% interface models. The interface region is magnified in (d). Like for the GaP/Si(111) interface [33], the averaged electrostatic potential shape of the GaP/Si(001) interface varies with atomic stoichiometry.

A complete list of the models is included in the Supplemental Material (Fig. SM-1 and Table SM-Tab.1) [43]. The charge neutrality condition [Eq. (8)] is fulfilled for c_{Si} equal to 8.3%, 16.7%, 25.0%, 33.3%, and 41.7%.

In Fig. 1, abrupt Si-P [Fig. 1(a)], abrupt Si-Ga [Fig. 1(b)], and selected mixed Si-Ga [Fig. 1(c)] and mixed Si-P [Figs. 1(d)–1(g)] interface structure models are shown. Each atomic slab consists of the (2×2) surface reconstruction, GaP epitaxial layers, interfacial layers, and Si bulk layers, as indicated in Fig. 1(c). The notation for the mixed model contains the Si concentration c_{Si} in the three GaP bilayers above the Si substrate (marked by the dashed rectangle in Fig. 1). For instance, Si substitution sites are presented in one and three GaP bilayers in Si-8.3% and Si-41.7% models, respectively [Figs. 1(c) and 1(g)].

The relaxed interplane distances were found to be different for Si-P and Si-Ga abrupt interfaces: 1.3 Å between Si and P layers [Fig. 1(a)] and 1.5 Å between Si and Ga layers [Fig. 1(b)]. These distances correspond to 5% contraction for the Si-P model and 10% expansion for the Si-Ga model with respect to the bulk Si interplane distance. Interplane distances between the mixed interfacial layers varied slightly with respect to the corresponding abrupt interface distances.

In Fig. 2, the relative interface formation energies are shown. The energy of the Si-8.3% model [Fig. 1(c)] was chosen as reference and set to zero. For clarity, the energy of the most stable mixed structure for each Si concentration and the energies of the two abrupt interfaces are shown in Fig. 2. Energies correspond to the interface models in Fig. 1. It is found that the compensated interface with Si/Ga substitution sites in the first interfacial layer is the most energetically favorable structure [Si-8.3% model in Fig. 1(c)], which is in agreement with our previous findings [6]. In addition, the interface energy increases with increasing Si concentration in
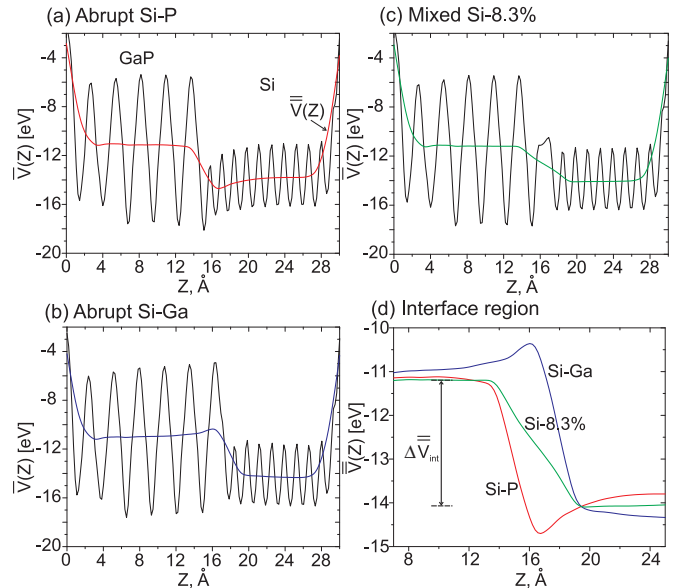
the GaP layers above the Si substrate. Therefore, although charge compensation can be realized by the Si/GaP atomic intermixture in the few layers above the interface, Si diffusion into the GaP(001) layers is energetically not favorable and should not occur in thermodynamical equilibrium.

Abrupt interfaces are less favorable than compensated interfaces, especially at chemical potentials in the intermediate range between Ga-rich and P-rich chemical potentials, around $\Delta\mu(P)/H_f = 0.5$. Therefore, abrupt interface preparation could be difficult at this condition. On the other hand, the formation of Si substitution sites is less favorable under the P-rich condition than under Ga-rich conditions.

Charge transfer due to heterovalent bonds is reflected in the electrostatic potential of the heterostructures. Figures 3(a)–3(c) show the planar average of electrostatic potentials $\bar{V}$ for abrupt Si-P, abrupt Si-Ga, and compensated Si-8.3% interface structures, respectively. The potential was averaged in plane (XY) over the unit-cell area and plotted along the [001] (Z) direction. The macroscopic average of the potential $\bar{\bar{V}}$ is shown by colored lines. In Fig. 3(d), the interface region is enlarged. There is a small residual slope of $\bar{\bar{V}}$ for the abrupt interfaces: Charge accumulates at the interface and produces a discontinuity of the electrostatic potential similar to other semiconductor interfaces [7]. This discontinuity of $\bar{\bar{V}}$ vanishes for compensated interfaces [Fig. 3(c), green line]: The electrostatic potential changes smoothly from GaP to Si at the compensated Si-8.3% interface, whereas there is a drastic potential variation at the Si-Ga and Si-P abrupt interfaces due to partial charge at the interface [Fig. 3(d)]. This charge can produce band bending at heterovalent uncompensated interfaces.

It is also important to mention that a dipole shift between the GaP and Si potentials, $\Delta\bar{\bar{V}}_{int}$ in Fig. 3(d), is present for

all considered interface models. In contrast, a complete dipole shift elimination was suggested for the Ge/GaAs(001) heterostructures with substitutional site defects in two interfacial layers (Fig. 4 in Ref. [4]). We cannot corroborate this effect for GaP/Si(001) mixed interfaces.

B. Core-level energy shifts at the interface

Core-level energy shifts due to heterovalent bonds at the interface are expected. Recently, the initial stages of GaP/Si(001) heterointerface formation and core-level binding energies of Ga, P, and Si atoms were investigated using XPS [10]. It was found that the P $2p$ and Si $2p$ core-level XPS peaks consist of two components, which were assigned to the interface and bulk contributions to the core-level photoelectron peak. The interface components were shifted towards higher binding energies relative to the bulk components. On the other hand, the Ga $2p$ peak only contained a weak, negatively shifted interface component at the initial stages of heterointerface formation at P-rich conditions [10]. A strong negative shift of the Ga $2p$ core level was observed for Si substrate preparation in Ga-rich conditions [8], but as these measurements were prior to nucleation, the magnitude of the shift is not directly comparable to the core-level shifts presented here.

The corresponding core-level binding energies and relative shifts were computed for the abrupt Si-Ga, the abrupt Si-P, and the lowest-energy Si-8.3% interface models. The difference in Si $2p$, P $2p$, and Ga $2p$ core-level binding energies $\Delta E = E_{int} - E_{bulk}$ was derived, where E_{int} and E_{bulk} are the binding energies of atoms at the interface (the first interfacial bilayer) and bulk, respectively. The bulk energies were computed using the atoms in the middle of Si or GaP slabs. The error bars of the computed binding energy were estimated from bulk binding-energy deviations: E_{bulk} slightly varies for the three models due to the limited thickness of the slabs and due to differences in the local electronic structure. The experimental error bars were obtained by variation of the Gaussian component fit parameters and by evaluation of the results. In addition, the experimental values of binding energies can be affected by the band bending due to surface reconstruction or contaminations. Therefore, the difference in binding energies ΔE was derived and compared with experimental values rather than the absolute binding energies.

In Fig. 4, the computed shifts ΔE for Si $2p$, P $2p$, and Ga $2p$ core levels for the abrupt Si-Ga [Fig. 4(a)], abrupt Si-P [Fig. 4(b)], and mixed Si-8.3% [Fig. 4(c)] models are compared with earlier experimental values [10]. There are Ga-P (P-Ga-P or Ga-P-Ga), Si-Si-Ga, Si-Si-P, Si-Ga-P (similar to Si-P-Ga), and Si-Si (Si-Si-Si) bonding configurations within one Si and one GaP bilayer at the interface. For abrupt interfaces, negative and positive binding-energy shifts are predicted for Si-Ga and Si-P models, respectively. In the case of the mixed interface, both positive and negative shifts are revealed. Experimental shifts derived from the P-polar interface are marked by the open rectangles. Note that no interface-related components in the Ga $2p$ core-level peak were measured [10]. The abrupt Si-P model thus agrees best with the experimental data, in line with our previous results and conclusions [10].
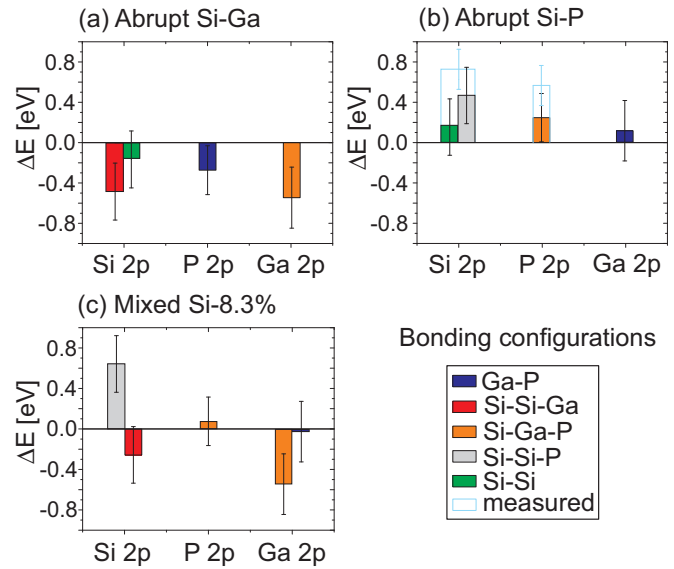

FIG. 4. Binding-energy shifts ΔE due to bonding configurations at the buried interface. The calculated values and experimental values [10] (for the abrupt Si-P interface only) of the shifts are marked by solid and open rectangles. (a) Negative and (b) positive shifts are predicted for the abrupt Si-Ga or Si-P interfaces, respectively. (c) The mixed interface exhibits both positive and negative shifts.

It should also be mentioned that experimental P and Ga core levels can contain contributions from the GaP(001)-(2 × 2) P dimer surface reconstruction. In addition, contamination or defects on the surface may contribute to P and Ga XPS peaks. From this point of view, the core-level peak shifts from buried Si atoms at the interface seem to be more suitable for the interface abruptness and polarity analysis: A mixture of Si-P and Si-Ga bonds causes both positive and negative shifts in the Si $2p$ bulk core level, so that three components in the Si $2p$ XPS peak are expected. The intensity of all Si $2p$ components should relate to the Si $2p$ cross section, so that the relative intensity of the two chemically shifted components (Si-Ga vs Si-P) can be considered a direct measure of the prevalence of the bonding type.

C. Interface electronic states

Surface and interface electronic states are expected at well-ordered surfaces and interfaces [14,24,31,44–46]. To identify these states for GaP/Si(001), the projected band structures (PBSs) of bulk GaP and Si were computed first and compared with GaP/Si(001) band structures. In Fig. 5, the PBSs of bulk Si and GaP are plotted within a (2 × 2) surface Brillouin zone [Fig. 5(c)]. There are pockets in the PBS that are free of bulk electronic states. In these regions, surface or interface states could relatively easily be identified. In the case of heterostructures, however, the Fermi energies of the two semiconductors are aligned, and the PBSs have to be shifted relative to each other by the VBO value [47].

VBOs of the abrupt [Figs. 1(a) and 1(b)] and the Si-8.3% [Fig. 1(c)] interface models were determined using the calculated shift of electrostatic potentials in the GaP/Si(001) heterostructure with respect to the corresponding values in GaP
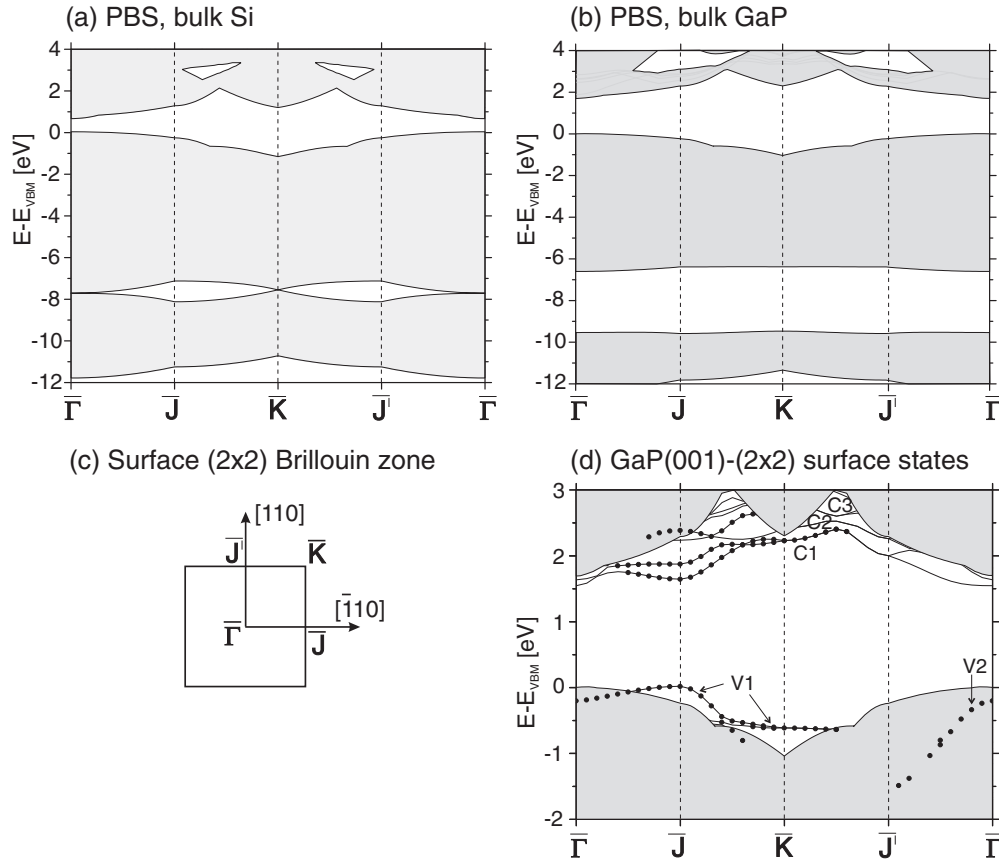
FIG. 5. Projected band structure of (a) bulk Si (light gray) and (b) bulk GaP (dark gray) within the (c) (2×2) Brillouin zone. The energy refers to the valence-band maximum. Surface states V1 and V2 in the valence band and C1–C3 in the conduction band are shown in (d). Surface states with high probability densities are indicated by black dots.

and Si bulk. The details of this method are described elsewhere [48,49]. The derived values are 0.32, 1.03, and 0.78 eV for the abrupt Si-Ga, Si-P, and Si-8.3% models, respectively. The GaP PBS was shifted downwards with respect to the Si PBS by these values (the Si valence-band maximum is set to zero). The joint bulk GaP/Si PBS is represented by shaded areas in Fig. 6.

It should be mentioned that there is an uncertainty in the VBO determination for abrupt uncompensated interfaces due to the discontinuity of the electrostatic potential [7]. The valence-band edge shifts with film thickness if an electrostatic field is present in a film [7,21]. In order to derive the VBO of abrupt interfaces, average point values of $\bar{\bar{V}}$ in the GaP and Si layers were used [Figs. 3(a) and 3(b)]. At these points, $\bar{\bar{V}}$ is almost flat, and the discontinuity can be neglected. For the compensated Si-8.3% interface, $\bar{\bar{V}}$ is saturated in the middle of GaP or Si layers, and therefore, VBO is determined explicitly.

The electronic states were identified by analyzing the layer-resolved squared wave functions of each band at a given **k** point of the heterointerface band structure [21]. Surface and interface states were separated from bulk states by the following analysis [50]:

$$\rho(\mathbf{k}, \text{band}) = \langle \rho_d \rangle^2 / \langle \rho_{\text{total}} \rangle, \qquad (9)$$

where $\langle \rho_d \rangle$ is an average of the probability density in a slab with thickness d (P dimer layer for surfaces and interface layers for heterostructures) and $\langle \rho_{\text{total}} \rangle$ is the average of the

total probability density in the whole heterostructure. $\langle \rho_d \rangle$ was squared in order to enhance the probability with respect to the bulk one. A 20% cutoff of the maximum of $\rho(\mathbf{k}, \text{band})$ was used to identify the states with enhanced probability density: States with probabilities below the cutoff were omitted [24]. This method enables a clear identification of the localized electronic states at selected layers of a slab.

The surface states of the GaP(001)-(2×2) surface reconstruction were analyzed first. In Fig. 5(d), electronic states of the (2×2) reconstruction are shown. The surface states V1 in the valence band and C1, C2, and C3 in the conduction band were clearly resolved. The dispersion of the states and the shape of the corresponding atomic orbitals (not shown here) agree well with previous calculations [31]. Enhanced probability densities $\rho(\mathbf{k}, \text{band})$ (Eq. (9)) for the given surface states are marked by black dots. In addition to the known surface states [31], one more resonant surface state, V2, was identified.

Surface states can overlap with interface states in heterostructures and complicate interface-state analysis. To exclude the surface states from an experimental analysis, they can easily be destroyed by surface contaminations or sputtering, for instance, whereas buried interface states will be preserved. Therefore, interface states were analyzed separately from the surface states.

Figures 6(a)–6(c) show electronic states close to the band gap of the heterostructure for abrupt Si-P, abrupt Si-Ga, and mixed Si-8.3% structure models, respectively. Light and dark
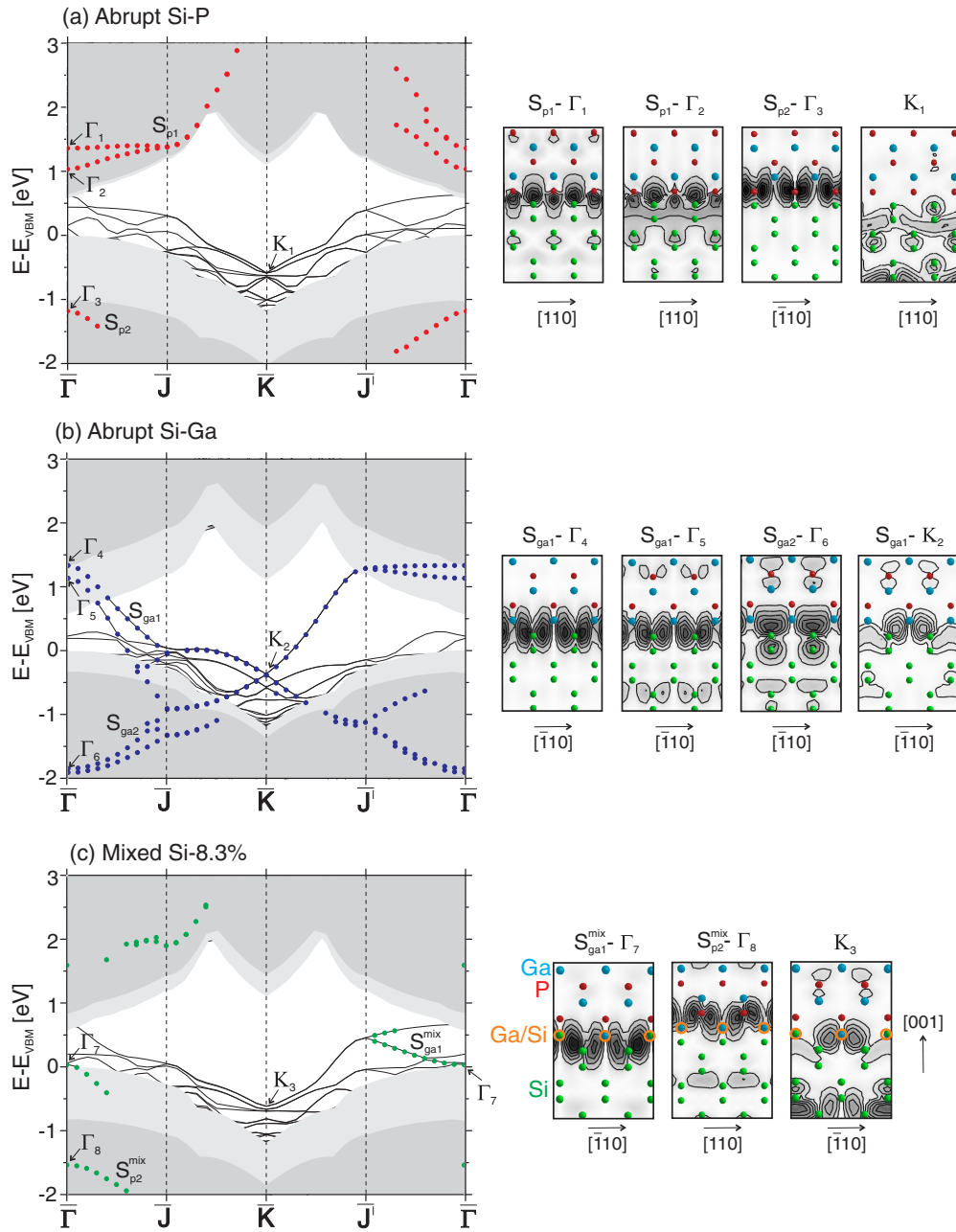
FIG. 6. Band structure and orbital character of the states for (a) abrupt Si-P, (b) abrupt Si-Ga, and (c) mixed Si-8.3% interface models. The joint PBS of bulk Si (light gray shading) and bulk GaP (dark gray shading) are shifted by the VBO value. States with high probability densities are shown by dots, whereas states in a band-gap region are shown by solid lines. Probability densities of surface states are omitted, but their state dispersion is similar to Fig. 5(c). The mixed Ga/Si layer is indicated by orange circles.

gray shaded areas correspond to the bulk Si and bulk GaP PBSs, respectively (shifted with respect to each other by the VBO values). The states, which overlap with the PBSs, are not shown except for interface states with a high probability density. Since states are present in the common band gap, the valence-band maximum (VBM) cannot clearly be seen. The valence-band edge was determined by extrapolation of the slope of the total density of states (DOS) at the beginning of the valence band (see Fig. SM-2 in the Supplemental Material). All bands were aligned to the edge of the VBM, which was determined with an estimated error bar of ± 0.1 eV.

There are surface and interface states above the VBM. Interface states can originate at Ga(P)-Si interface layers as well as at Si layers below the interface plane. The latter states do not completely overlap with the PBS due to atomic relaxations in heterostructure. In particular for the abrupt Si-P heterostructure, there are no interface states with a high probability density (dots), which are localized at only the Si-P interface plane [Fig. 6(a)]. The interface states of Si layers and surface states are present, however (black lines). The interface states due to P-Si bonds (dots) overlap with the PBS and, unfortunately, are hard to be resolved experimentally.

There are distinct features in the state dispersion for the abrupt Si-P and Si-Ga interfaces. In particular, the S_{ga1} interface state with a high probability density lies in the common band gap of the abrupt Si-Ga heterostructure [Fig. 6(b)], whereas no such interface state is present for the abrupt Si-P heterostructure: The pronounced state dispersion along the $\bar{K} - \bar{J}'$ direction is distinct for the Si-Ga interface. This region of the band structure could be suitable for abrupt GaP/Si(001) interface polarity measurements.

Cross sections through the probability density at the $\bar{\Gamma}$ and $\bar{K}$ points are shown on the right-hand side of Fig. 6. The [001] cross-section planes are aligned along the [110] and [$\bar{1}$10] directions. It is seen that the $S_{p1,2}$ and the S_{ga1} states are mainly localized at the Si-P and Si-Ga interface bonds, respectively. On the other hand, interface states at the K_1 and K_3 points are localized at Si-Si bonds below the interface plane. Some interface states are split, but they have a similar orbital character; that is, $S_{p1} - \Gamma_1$ is similar to $S_{p1} - \Gamma_2$, and $S_{ga1} - \Gamma_4$ is similar to $S_{ga1} - \Gamma_5$.

Interface states of the mixed Si-8.3% model are shown in Fig. 6(c). ρ_d was computed in the middle of the Ga/Si atomic plane. In contrast to the abrupt interface states, interface state S_{ga1}^{mix} is in the common band gap of the PBS along the $\bar{J}'$-$\bar{\Gamma}$ points. This state overlaps with the Si substrate states close to the K_3 point. Similar to the abrupt interfaces, interface state S_{p2}^{mix} is below the VBM.

The cross section through the probability density of the mixed interface is shown in Fig. 6(c). The mixed Ga/Si layer is indicated by orange circles. The mixed interface orbital contour plots are quite similar to the corresponding plots of abrupt interfaces. In particular, the $S_{p2} - \Gamma_3$ (or $S_{ga1} - \Gamma_4$) plot is similar to the $S_{p2}^{mix} - \Gamma_8$ (or $S_{ga1}^{mix} - \Gamma_7$) plot. Despite the orbital characters of the mixed and abrupt GaP/Si(001) interfaces being similar, the dispersion of the interface states and their alignment with respect to the valence-band maximum are quite different.

It should finally be mentioned that the band structure calculations were carried out for ideally ordered GaP/Si(001) interfaces. Atomic disorder due to substitution-site diversity or ADBs can smear out or even completely destroy the interface-state dispersion in real heterostructures. On the other hand, experimental evidence of interface-state dispersion and its correlation with the present theoretical predictions would be a strong evidence for high atomic order at a heterovalent GaP/Si(001) interface.

IV. CONCLUSIONS

Atomic and electronic band structures of the GaP/Si(001) heterostructures terminated by the P-rich (2×2) surface reconstruction were investigated by *ab initio* DFT calculations. In addition to the abrupt Si-P and Si-Ga interface models, interface structures with Si substitution sites in three GaP bilayers above the Si substrate were considered. We found that some mixed interfaces exhibit lower energies than the abrupt interfaces in thermodynamical equilibrium. The lowest-energy interface model consists of one Si/Ga intermixed layer above the Si substrate. Diffusion of Si atoms into GaP(001) epitaxial layers above the first interface layer is energetically unfavorable. We also showed that Ga, P, and Si $2p$ core-level energies are shifted to higher or lower binding energies due to heterovalent Si-P or Si-Ga bonds at the interface, respectively. For the mixed interface, the Si $2p$ XPS peak should consist of positively and negatively shifted components with respect to the bulk Si $2p$ binding energy. Band structure calculations revealed interface states in the common band gap of two semiconductors above the VBM. The predicted dispersion of the GaP/Si(001) interface states is anisotropic and provides distinct features for further experimental interface polarity studies.

[1] J. A. del Alamo, Nature (London) **479**, 317 (2011).

[2] M. M. May, H.-J. Lewerenz, D. Lackner, F. Dimroth, and T. Hannappel, Nat. Commun. **6**, 8286 (2015).

[3] N. Nakagawa, H. Y. Hwang, and D. A. Muller, Nat. Mater. **5**, 204 (2006).

[4] W. A. Harrison, E. A. Kraut, J. R. Waldrop, and R. W. Grant, Phys. Rev. B **18**, 4402 (1978).

[5] H. Kroemer, J. Cryst. Growth **81**, 193 (1987).

[6] O. Supplie, S. Brückner, O. Romanyuk, H. Döscher, C. Höhn, M. M. May, P. Kleinschmidt, F. Grosse, and T. Hannappel, Phys. Rev. B **90**, 235301 (2014).

[7] A. Kley and J. Neugebauer, Phys. Rev. B **50**, 8616 (1994).

[8] O. Supplie, M. M. May, C. Höhn, H. Stange, A. Müller, P. Kleinschmidt, S. Brückner, and T. Hannappel, ACS Appl. Mater. Interfaces **7**, 9323 (2015).

[9] S. Brückner, H. Döscher, P. Kleinschmidt, O. Supplie, A. Dobrich, and T. Hannappel, Phys. Rev. B **86**, 195310 (2012).

[10] O. Supplie, M. M. May, G. Steinbach, O. Romanyuk, F. Grosse, A. Nägelein, P. Kleinschmidt, S. Brückner, and T. Hannappel, J. Phys. Chem. Lett. **6**, 464 (2015).

[11] R. D. Bringans, M. A. Olmstead, R. I. G. Uhrberg, and R. Z. Bachrach, Phys. Rev. B **36**, 9569 (1987).

[12] A. Beyer, A. Stegmüller, J. O. Oelerich, K. Jandieri, K. Werner, G. Mette, W. Stolz, S. D. Baranovskii, R. Tonner, and K. Volz, Chem. Mater. **28**, 3265 (2016).

[13] T. Hannappel, O. Supplie, S. Brückner, M. M. May, P. Kleinschmidt, and O. Romanyuk, arXiv:1610.01758 [cond-mat.mtrl-sci].

[14] G. Margaritondo, Rep. Prog. Phys. **62**, 765 (1999).

[15] T. Yasuda, Thin Solid Films **313**, 544 (1998).

[16] O. Supplie, T. Hannappel, M. Pristovsek, and H. Döscher, Phys. Rev. B **86**, 035308 (2012).

[17] L. Esaki, W. Howard, and J. Heer, Surf. Sci. **2**, 127 (1964).

[18] A. Franciosi and C. G. V. de Walle, Surf. Sci. Rep. **25**, 1 (1996).

[19] J. E. Rowe, S. B. Christman, and G. Margaritondo, Phys. Rev. Lett. **35**, 1471 (1975).

[20] T. Saito and T. Ikoma, Phys. Rev. B **45**, 1762 (1992).

[21] M. Di Ventra, C. Berthod, and N. Binggeli, Phys. Rev. B **71**, 155324 (2005).

[22] J. Pollmann and S. T. Pantelides, Phys. Rev. B **21**, 709 (1980).

[23] F. G. Margaritondo, G. Cerrina, F. Capasso, C. Patella, F. Perfetti, P. Quaresima, and C. Grunthaner, Solid State Commun. **52**, 495 (1984).

[24] M. Peressi, F. Fovot, G. Cangiani, and A. Baldereschi, Appl. Phys. Lett. **81**, 5171 (2002).

[25] G. Steinbach, M. Schreiber, and S. Gemming, Nanosci. Nanotech. Lett. **4**, 1 (2012).

[26] X. Gonze, J.-M. Beuken, R. Caracas, F. Detraux, M. Fuchs, G.-M. Rignanese, L. Sindic, M. Verstraete, G. Zerah, F. Jollet, *et al.*, Comput. Mater. Sci. **25**, 478 (2002).

[27] X. Gonze, G.-M. Rignanese, M. Verstraete, J.-M. Beuken, Y. Pouillon, R. Caracas, F. Jollet, M. Torrent, G. Zerah, M. Mikami *et al.*, Z. Kristallogr. **220**, 558 (2005).

[28] M. Fuchs and M. Scheffler, Comput. Phys. Commun. **119**, 67 (1999).

[29] N. Troullier and J. L. Martins, Phys. Rev. B **43**, 1993 (1991).

[30] H. J. Monkhorst and J. D. Pack, Phys. Rev. B **13**, 5188 (1976).

[31] P. H. Hahn, W. G. Schmidt, F. Bechstedt, O. Pulci, and R. Del Sole, Phys. Rev. B **68**, 033311 (2003).

[32] P. Sippel, O. Supplie, M. M. May, R. Eichberger, and T. Hannappel, Phys. Rev. B **89**, 165312 (2014).

[33] O. Romanyuk, T. Hannappel, and F. Grosse, Phys. Rev. B **88**, 115312 (2013).

[34] M. Bernasconi, G. L. Chiarotti, and E. Tosatti, Phys. Rev. B **52**, 9988 (1995).

[35] Y. Takao and A. Morita, Phys. B (Amsterdam, Neth.) **105**, 93 (1981).

[36] V. Kumar and B. S. R. Sastry, Phys. Stat. Sol. **242**, 869 (2005).

[37] C. E. Dreyer, A. Janotti, and C. G. Van de Walle, Phys. Rev. B **89**, 081305(R) (2014).

[38] H. Li, L. Geelhaar, H. Riechert, and C. Draxl, Phys. Rev. Lett. **115**, 085503 (2015).

[39] M. P. Ljunberg, J. J. Mortenson, and L. G. M. Pettersson, J. Electr. Spectrosc. Relat. Phenom. **184**, 427 (2011).

[40] T. Susi, D. J. Mowbray, M. P. Ljungberg, and P. Ayala, Phys. Rev. B **91**, 081401(R) (2015).

[41] J. Enkovaara, C. Rostgaard, J. J. Mortensen, J. Chen, M. Dulak, L. Ferrighi, J. Gavnholt, C. Glinsvad, V. Haikola, and H. A. Hansen, J. Phys. Condens. Matter **22**, 253202 (2010).

[42] M. D. Pashley, Phys. Rev. B **40**, 10481 (1989).

[43] See Supplemental Material at http://link.aps.org/supplemental/10.1103/PhysRevB.94.155309 for a list of structure models and density of states of the heterostructures.

[44] W. E. Pickett, S. G. Louie, and M. L. Cohen, Phys. Rev. Lett. **39**, 109 (1977).

[45] W. E. Pickett and M. L. Cohen, Phys. Rev. B **18**, 939 (1978).

[46] *Characterization of Semiconductor Heterostructures and Nanostructures*, 2nd ed., edited by G. Agostini and C. Lamberti (Elsevier, Oxford, 2013).

[47] C. Huang, L. Ye, and X. Wang, J. Phys. Condens. Matter **1**, 907 (1989).

[48] J. von Pezold and P. D. Bristowe, J. Mater. Sci. **40**, 3051 (2005).

[49] K. Steiner, W. Chen, and A. Pasquarello, Phys. Rev. B **89**, 205309 (2014).

[50] O. Romanyuk, K. Hattori, M. Someta, and H. Daimon, Phys. Rev. B **90**, 155305 (2014).